Article

Journal of Vibration and Control
1–10

DOI: 10.1177/1077546316688992
journals.sagepub.com/home/jvc
SAGE

Robust and adaptive control of coexisting attractors in nonlinear vibratory energy harvesters

Ashkan Haji Hosseinloo[1], Jean-Jacques Slotine[1,2] and Konstantin Turitsyn[1]

Abstract

An immense body of research has focused on nonlinear vibration energy harvesting systems mainly because of the inherent narrow bandwidth of their linear counterparts. However, nonlinear systems driven by harmonic excitation often exhibit coexisting periodic or chaotic attractors. For effective energy harvesting, it is always desired to operate on the high-energy periodic orbits; therefore, it is crucial for the harvester to move to the desired attractor once the system is trapped in any other coexisting attractor. Here we propose a robust and adaptive sliding mode controller to move the nonlinear harvester to any desired attractor by a short entrainment on the desired attractor. The proposed controller is robust to disturbances and unmodeled dynamics and adaptive to the system parameters. The results show that the controller can successfully move the harvester to the desired attractor, even when the parameters are unknown, in a reasonable period of time, in less than 30 cycles of the excitation force.

Keywords

Nonlinear energy harvesting, coexisting attractors, bistable potential, sliding mode control, robust, adaptive

1. Introduction

The narrow bandwidth of linear vibratory energy harvesters has convinced researchers to exploit nonlinearity to broaden the harvesting bandwidth (Hosseinloo and Turitsyn, 2015a; Hosseinloo et al., 2015). However, nonlinearity often brings with it coexisting chaotic or periodic attractors, which are, in general, undesired. In the context of energy harvesting, monostable and bistable quartic potentials are by far the most common type of nonlinearity explored in the literature.

Nonlinear monostable harvesters driven by periodic excitation often exhibit coexisting low- and high-amplitude orbits, usually referred to as low- and high-energy orbits, over a wide range of excitation frequencies. Bistable harvesters give rise to even richer dynamics where low- and high-energy periodic and chaotic attractors could coexist in a wide range of excitation parameters (Daqaq et al., 2014; Hosseinloo and Turitsyn, 2015b). For the purpose of energy harvesting, it is always desired to surf the high-energy periodic orbits. If the motion is chaotic, in addition to its low-energy output relative to high-energy orbit motion, the chaotic response requires a more complicated harvesting circuitry (Erturk and Inman, 2011). Therefore, control of the motion between the coexisting attractors in vibratory energy harvesters is extremely important for effective harvesting.

In a seminal studies in controlling chaos, Ott et al. (1990) showed that one can convert a chaotic attractor to any one of the possible but probably unstable time-periodic motions by making only small time-dependent perturbations to an available and accessible system parameter. This approach is known as the

[1]Department of Mechanical Engineering, Massachusetts Institute of Technology, USA
[2]Department of Brain and Cognitive Sciences, Massachusetts Institute of Technology, USA

Received: 19 May 2016; accepted: 5 November 2016

Corresponding author:
Ashkan Haji Hosseinloo, Department of Mechanical Engineering, Massachusetts Institute of Technology, Cambridge, Massachusetts 02139, USA.
Email: ashkanhh@mit.edu

Ott–Grebogi–Yorke method. Later, Pisarchik and Goswami (Pisarchik and Goswami, 2000; Pisarchik, 2001; Goswami and Pisarchik, 2008) used a slow-periodic modulation with properly adjusted frequency and amplitude, instead of just a small perturbation, to move to an adjacent attractor via boundary crises and destruction of the original attractor.

However, the parameters of the system are not always accessible; hence, the Ott–Grebogi–Yorke method is not always practical. Periodic driving is another technique for the control of coexisting attractors. Pecora and Carroll (1991) used what they called pseudoperiodic signals, i.e. periodic signals augmented with a small chaotic component, to control the coexisting attractors. Yang et al. (1995) used a combination of noise and a bias periodic signal with a properly chosen phase to move the attractor to a desired limit cycle.

Feedback-type control is another method of controlling coexisting attractors. Jiang (1999) showed that the main feature of the latter two aforementioned methods is the periodic component of their signals and that both approaches have limitations in selecting a desired trajectory from arbitrary initial conditions. Jiang used feedback-type periodic drivers containing dynamical features of the desired attractors to control the attractors and switch to the desired cycle. Martinez-Zerega et al. (2003) also demonstrated that multistability can be efficiently controlled in autonomous systems by modulating feedback variables. More recently, Liu et al. (2013) proposed a feedback controller with intermittent control force based on Lyapunov analysis to drive the system to a desired attractor.

Although some of these methods could be theoretically applied to nonlinear energy harvesters, they do not take into account the control energy, which is crucial in designing the controller for the vibratory energy harvesters. Also most of these approaches use some type of crisis that changes the existing structure of the solutions. This is, in general, not preferred because not only could it be hard to achieve for some nonlinear systems but it could also result in the emergence of new complex basins of attraction (Liu et al., 2013). There are very few studies in the context of energy harvesting dealing with the control of coexisting attractors, a ubiquitous phenomenon in nonlinear energy harvesters.

Erturk and Inman (2011), in one of the earliest research studies, showed that a disturbance could push the vibratory energy harvester from a low-energy orbit to a high-energy orbit. Masuda et al. (2013) proposed an electrical circuitry for an electromagnetic vibratory energy harvester that combined a conventional load resistance with a negative resistance that could pump energy into the system. In their proposed approach, when the amplitude drops below a threshold, the circuit switches to the negative resistance for a given period of time to push the system back to the high-energy orbit. This was later validated experimentally by Masuda and Sato (2016). This approach will not be effective when the structure of the coexisting attractors is more complex than two periodic orbits, mainly because it cannot select between many chaotic or periodic attractors in a controlled fashion. In another study, Geiyer and Kauffman (2016) applied the intermittent control law proposed by Liu et al. (2013) to a piezoelectric vibratory energy harvester to drive the system from a chaotic attractor to a high-energy periodic motion. However, the control energy was not considered in this study. In a more recent study, Kumar et al. (2016) applied a linear quadratic regulation controller to a bistable piezoelectric energy harvester linearized about an operating point corresponding to a chosen high-energy orbit. The linear quadratic regulation control force was applied intermittently to the system based on a proximity threshold with respect to the desired trajectory. The required control energy was not compared with the harvested energy in this study either.

In addition to the already-mentioned shortcomings of the proposed methods for driving nonlinear vibratory energy harvesters to their high-energy orbits, these methods are in general neither robust nor adaptive. In practical applications of the vibratory energy harvesters, there are always disturbances or unmodeled dynamics on the system, such as wind disturbance on a bridge-motion-excited vibratory energy harvester or unmodeled higher-order nonlinearities in the system. Also, it is usually the case that some system parameters, such as damping or coupling factors, are not accurately or deterministically known or that they may change over time due to wear and tear or environmental conditions (Hosseinloo and Turitsyn, 2016a,b). Therefore, it is very advantageous if the controller is robust to external disturbances and unmodeled dynamics and, of course, if it is adaptive, i.e. it works even when the system parameters are unknown. In this study, we propose a generic robust and adaptive sliding mode control that can drive the system from any attractor to any other stable attractor of interest. It is shown that the control energy budget is recovered by the harvested energy within a reasonable period of time.

2. Mathematical modeling of the nonlinear harvester

In this section, we present a simple formulation of piezoelectric and electromagnetic energy harvesters with generic nonlinearity. Here, we consider a vibratory energy harvester with a second-order mechanical oscillator and a first-order electronic circuitry (capacitive or inductive). The governing dynamics equations could

be written as

$$\begin{aligned} m\bar{x}'' + \bar{f}(\bar{x},\bar{x}',\bar{y},\bar{t}) &= \bar{F}(\bar{t}) + \bar{d}_1(\bar{t}) + \bar{u}_{\mathrm{m}}(\bar{t}) \\ C_{\mathrm{p}}\bar{y}' + \bar{g}(\bar{x},\bar{x}',\bar{y},\bar{t}) &= \bar{d}_2(\bar{t}) + \bar{u}_{\mathrm{e}}(\bar{t}) \quad \text{(piezoelectric)} \\ L\bar{y}' + \bar{g}(\bar{x},\bar{x}',\bar{y},\bar{t}) &= \bar{d}_2(\bar{t}) + \bar{u}_{\mathrm{e}}(\bar{t}) \quad \text{(electromagnetic)} \end{aligned} \tag{1}$$

where, m, C_{p}, and L are the oscillator mass, the inherent capacitance of the capacitive circuit, and the inductance of the inductive circuit, respectively. $(.)'$ denotes the derivative with respect to time $\bar{t}$. $\bar{x}$ and $\bar{y}$ are the oscillator displacement and electrical state (voltage for capacitive and current for inductive circuitry). $\bar{F}(\bar{t})$ represents external excitation on the system, and $\bar{d}_1(\bar{t})$ and $\bar{d}_2(\bar{t})$ denote unmodeled dynamics or disturbances in the mechanical and electrical domains, respectively. $\bar{u}_{\mathrm{m}}(\bar{t})$ and $\bar{u}_{\mathrm{e}}(\bar{t})$ represent the control forces on the mechanical oscillator and the electrical circuit, respectively. All other dynamics in the mechanical and electrical domains are embedded in $\bar{f}(.)$ and $\bar{g}(.)$, respectively. This includes all the system nonlinearities and electromechanical couplings. For instance, for a vibratory energy harvester with linear damping (c) and generic potential function $\bar{U}(\bar{x})$ coupled with a linear piezoelectric or electromagnetic circuitry (with linear electromechanical coupling θ) connected to a load resistance R, the $\bar{f}$ and $\bar{g}$ functions will be

$$\begin{aligned} \bar{f} &= c\bar{x}' + \mathrm{d}\bar{U}(\bar{x})/\mathrm{d}\bar{x} + \theta\bar{y} \\ \bar{g} &= \frac{\bar{y}}{R} - \theta\bar{x}' \quad \text{(piezoelectric)} \\ \bar{g} &= R\bar{y} - \theta\bar{x}' \quad \text{(electromagnetic)} \end{aligned} \tag{2}$$

To unify the analysis for the capacitive and inductive circuitry and to reduce the number of the parameters, we nondimensionalize the governing equations. A meaningful nondimensionalization usually depends on the parameters of the system. Assuming that we have a dimensional parameter θ with units of newtons per volt (newtons per ampere) for a capacitive (inductive) harvester, we can nondimensionalize equation (1) using the following dimensionless quantities

$$\begin{aligned} x &= \frac{\bar{x}}{l_{\mathrm{s}}}, \quad t = \bar{t}\omega_{\mathrm{s}}, \\ y &= \frac{C_{\mathrm{p}}}{\theta l_{\mathrm{s}}}\bar{y} \quad \text{(piezoelectric)} \\ y &= \frac{L}{\theta l_{\mathrm{s}}}\bar{y} \quad \text{(electromagnetic)} \end{aligned} \tag{3}$$

where l_{s} and ω_{s} define length and time scales, respectively. Then the governing equations in equation (1) could be nondimensionalized as

$$\begin{aligned} \ddot{x} + f(x,\dot{x},y,t) &= F(t) + d_1(t) + u_{\mathrm{m}}(t) \\ \dot{y} + g(x,\dot{x},y,t) &= d_2(t) + u_{\mathrm{e}}(t) \end{aligned} \tag{4}$$

where the overbars are dropped to designate the corresponding dimensionless variables and functions. $(\dot{.})$ denotes the derivative with respect to the dimensionless time t.

3. Robust and adaptive sliding mode control

Its inherent robustness and adaptation capability makes sliding mode control a suitable candidate for many control applications where there are unmodeled dynamics and disturbances, and when the system parameters are unknown. For these reasons, we will use adaptive sliding mode control here to control the attractors of a nonlinear vibratory energy harvester or, in particular, to drive the harvester to a high-energy attractor. Since the energy budget for the controller is important for energy harvesting purposes, and since the desired trajectories are always attractors, we do not need the controller to act for all time. In fact, we use the controller to entrain the system along the desired trajectory for a short period of time to make sure that all the transients are settled and that the system is in the new desired basin of attraction before we turn off the controller.

To this end, we first transform the higher-order dynamics to first-order dynamics by a change of variable. The new variables, often referred to as sliding surfaces, should have two important properties: (i) their derivatives should contain the control forces, and (ii) the new variables going to zero should imply that the actual states of the system converge to the desired states. Then we design the controller to push the sliding surface to zero, and hence make the system track the desired trajectory, i.e. the high-energy orbit.

We first define the sliding surface vector $\mathbf{s} = [s_1, s_2]^{\mathrm{T}} = [\dot{\tilde{x}} + \lambda\tilde{x}, \tilde{y}]^{\mathrm{T}}$, where $\lambda > 0$, $\tilde{x} = x - x_{\mathrm{d}}$ and $\tilde{y} = y - y_{\mathrm{d}}$. $x_{\mathrm{d}}(t)$ and $y_{\mathrm{d}}(t)$ are the desired displacement and electrical state trajectories. Also let $\mathbf{a}$ denote the vector of unknown parameters and $\hat{\mathbf{a}}$ represent the vector of estimated parameters. We also assume that each of the functions f and g could be written as the product of a row matrix and the parameters vector i.e. $f = \mathbf{Y_1 a}$ and $g = \mathbf{Y_2 a}$. The elements of $\mathbf{Y_1}$ and $\mathbf{Y_2}$ will be linear or nonlinear functions of the states of the harvester and the time. We can also safely assume that the disturbances or the unmodeled dynamics are bounded, that is $|d_1| < d_1^{\max}$ and $|d_2| < d_2^{\max}$.

Theorem 1. For the nonlinear vibratory energy harvester with the governing equations stated in equation (), the harvester will converge to the desired attractor, i.e. $x \to x_d$ and $y \to y_d$ if the control law is chosen as

$$\begin{aligned} u_m &= -F(t) + \ddot{x}_d - \lambda(\dot{x} - \dot{x}_d) + \mathbf{Y}_1\widehat{\mathbf{a}} \\ &\quad - (\eta_1 + d_1^{\max})\text{sign}(s_1) \\ u_e &= \dot{y}_d + \mathbf{Y}_2\widehat{\mathbf{a}} - (\eta_2 + d_2^{\max})\text{sign}(s_2) \end{aligned} \tag{5}$$

and the adaptation law is chosen as

$$\dot{\widehat{\mathbf{a}}} = -\mathbf{P}\mathbf{Y}^{\mathrm{T}}\mathbf{s} \tag{6}$$

where $\eta_1 > 0$ and $\eta_2 > 0$ are two positive real gains, and $\mathbf{P}$ is a symmetric positive definite matrix defining the adaptation gains. $\mathbf{Y}$ is simply $[\mathbf{Y_1}, \mathbf{Y_2}]^{\mathrm{T}}$.

Proof. As is typical for most sliding mode control problems, the proof is based on Barbalat's lemma for stability analysis. Let us consider the lower-bounded Lyapunov-like energy function $V(\mathbf{s}, t)$ as

$$V(\mathbf{s}, t) = \frac{1}{2}\mathbf{s}^{\mathrm{T}}\mathbf{s} + \frac{1}{2}\widetilde{\mathbf{a}}^{\mathrm{T}}\mathbf{P}^{-1}\widetilde{\mathbf{a}} \tag{7}$$

where $\widetilde{\mathbf{a}} = \widehat{\mathbf{a}} - \mathbf{a}$. In view of Barbalat's lemma, if $\dot{V}(\mathbf{s}, t)$ is negative semi-definite, and uniformly continuous in time, then $\dot{V}(\mathbf{s}, t) \to 0$ as $t \to \infty$ (Slotine and Li, 1991). We will show that with the choice of control and adaptation laws as in equations (5) and (6), not only is $\dot{V}(\mathbf{s}, t) \to 0$ but it also implies that the sliding surface vector goes to zero ($\mathbf{s} \to \mathbf{0}$), which consequently means that the harvester converges to the desired trajectory or attractor. To do so, let us differentiate the function $V(\mathbf{s}, t)$ and substitute the sliding surface and also the dynamics $\ddot{x}$ and $\dot{y}$ from equation (4)

$$\begin{aligned} \dot{V}(\mathbf{s}, t) &= s_1\dot{s}_1 + s_2\dot{s}_2 + \dot{\widetilde{\mathbf{a}}}^{\mathrm{T}}\mathbf{P}^{-1}\widetilde{\mathbf{a}} \\ &= s_1(\ddot{x} - \ddot{x}_d + \lambda(\dot{x} - \dot{x}_d)) + s_2(\dot{y} - \dot{y}_d) \\ &\quad + \dot{\widehat{\mathbf{a}}}^{\mathrm{T}}\mathbf{P}^{-1}\widetilde{\mathbf{a}} \\ &= s_1(u_m + F + d_1 - \ddot{x}_d + \lambda(\dot{x} - \dot{x}_d) - f) \\ &\quad + s_2(u_e + d_2 - \dot{y}_d - g) + \dot{\widehat{\mathbf{a}}}^{\mathrm{T}}\mathbf{P}^{-1}\widetilde{\mathbf{a}} \end{aligned} \tag{8}$$

Now we substitute the control law (equation (5)) into equation (8) and rewrite the functions f and g as the product of their corresponding row matrices and the vector of parameters. Hence

$$\begin{aligned} \dot{V}(\mathbf{s}, t) &= s_1(d_1 - (d_1^{\max} + \eta_1)\text{sign}(s_1) + \mathbf{Y}_1\widetilde{\mathbf{a}}) \\ &\quad + s_2(d_2 - (d_2^{\max} + \eta_2)\text{sign}(s_2) + \mathbf{Y}_2\widetilde{\mathbf{a}}) \\ &\quad + \dot{\widehat{\mathbf{a}}}^{\mathrm{T}}\mathbf{P}^{-1}\widetilde{\mathbf{a}} \end{aligned} \tag{9}$$

Finally, we substitute the adaptation law (equation (6)) into equation (9) to get

$$\begin{aligned} \dot{V}(\mathbf{s}, t) &= s_1\big(d_1 - d_1^{\max}\text{sign}(s_1)\big) - \eta_1 s_1\text{sign}(s_1) \\ &\quad + s_2(d_2 - d_2^{\max}\text{sign}(s_2)) - \eta_2 s_2\text{sign}(s_2) \\ &\le -\eta_1|s_1| - \eta_2|s_2| \le 0 \end{aligned} \tag{10}$$

We have shown that the lower-bounded function $V(\mathbf{s}, t)$ has a negative semi-definite derivative. Technically, we still need to show that this derivative is uniformly continuous in time. A very simple sufficient condition for a differentiable function to be uniformly continuous is that its derivative be bounded. Therefore, it is sufficient to show that $\ddot{V}(\mathbf{s}, t)$ is bounded to complete the proof. This second derivative includes $\dot{\mathbf{s}}$ and so we need to show that $\dot{\mathbf{s}}$ is bounded. Notice that $V(\mathbf{s}, t)$ is the sum of two positive numbers and its derivative is negative; hence, it is bounded by its initial value, which implies that $\mathbf{s}$ and $\widetilde{\mathbf{a}}$ are bounded, which means that the system states are bounded. $\dot{\mathbf{s}}$ being bounded requires that $\dddot{y}$, $\dddot{x}$, and $\dddot{\bar{x}}$ be bounded, which consequently implies that $\dot{y}$, $\dot{x}$, and $\ddot{x}$ be bounded, assuming that the desired trajectories are bounded. Having the states of the system bounded, and in view of the system dynamics (equation (4)), it can be seen that $\dot{y}$ and $\ddot{x}$ are bounded.

Therefore, $\dot{\mathbf{s}}$ is bounded. Fulfilling the three requirements of Barbalat's lemma, the proof is completed and we can conclude that $\dot{V}(\mathbf{s}, t) \to 0$. In view of equation (10), this means that $\mathbf{s} \to \mathbf{0}$, i.e. the system converges to the desired attractor.

3.1. Bistable energy harvester

Here, we consider a more specific design of the nonlinear vibratory energy harvester; a bistable energy harvester, one of the most common nonlinear vibratory energy harvesters in the literature. If we use the bistable potential $\bar{U}(\bar{x}) = 1/2k_1\bar{x}^2 + 1/4k_3\bar{x}^4$ for the potential function in equation (2), substitute equation (2) into equation (1), and nondimensionalize using the quantities in equation (3), we arrive at the dimensionless governing equations as

$$\begin{aligned} \ddot{x} + 2\zeta\dot{x} - x + x^3 + \kappa^2 y &= F(t) + d_1(t) + u_m(t) \\ \dot{y} + \alpha y &= \dot{x} + d_2(t) + u_e(t) \end{aligned} \tag{11}$$

where $\zeta = c/2m\omega_s$ is the dimensionless damping ratio. The electromechanical coupling coefficient κ^2 and the time ratio (mechanical to electrical time constants) α for piezoelectric and electromagnetic harvesters are defined as

$$\begin{aligned} \kappa^2 &= \frac{\theta^2}{m\omega_s^2 C_p}, \quad \alpha = \frac{1}{RC_p\omega_s} \quad \text{(piezoelectric)} \\ \kappa^2 &= \frac{\theta^2}{m\omega_s^2 L}, \quad \alpha = \frac{R}{L\omega_s} \quad \text{(electromagnetic)} \end{aligned} \tag{12}$$

The dimensional coefficients k_1 and k_3 for the potential function are chosen such that the derivative of the potential function in the dimensionless form is $-x + x^3$.

To design the sliding mode controller, we assume that the two parameters ζ and κ^2 are unknown, i.e. $\mathbf{a} = [\zeta, \kappa^2]^{\mathrm{T}}$. Also, we choose $\mathbf{P}$, a diagonal matrix, as $\mathbf{P} = \mathrm{diag}[p_1, p_2]$ with positive entries p_1 and p_2. Then applying equation (5) yields the control forces as

$$\begin{aligned} u_{\mathrm{m}} &= -F(t) + \ddot{x}_{\mathrm{d}} - \lambda(\dot{x} - \dot{x}_{\mathrm{d}}) - x + x^3 + 2\hat{\zeta}\dot{x} + \hat{\kappa}^2 y \\ &\quad - (\eta_1 + d_1^{\max})\mathrm{sign}(s_1) \\ u_{\mathrm{e}} &= -\dot{x} + \alpha y + \dot{y}_{\mathrm{d}} - \left(\eta_2 + d_2^{\max}\right)\mathrm{sign}(s_2) \end{aligned} \tag{13}$$

and the adaptation law forms into

$$\begin{aligned} \dot{\hat{\zeta}} &= -2p_1 \dot{x} s_1 \\ \dot{\hat{\kappa}}^2 &= -p_2 y s_1 \end{aligned} \tag{14}$$

We would also like to nondimensionalize the harvested and the controller power and their corresponding energies. The power is made dimensionless by the quantity $mw_{\mathrm{s}}^3 l_{\mathrm{s}}^2$ as

$$\begin{aligned} P_{\mathrm{h}}(t) &= \frac{\bar{P}_{\mathrm{h}}(\bar{t})}{mw_{\mathrm{s}}^3 l_{\mathrm{s}}^2} = \alpha\kappa^2 y^2(t) \\ P_{\mathrm{m}}(t) &= \frac{\bar{P}_{\mathrm{m}}(\bar{t})}{mw_{\mathrm{s}}^3 l_{\mathrm{s}}^2} = \frac{\bar{u}_{\mathrm{m}}(\bar{t})\bar{x}'(\bar{t})}{mw_{\mathrm{s}}^3 l_{\mathrm{s}}^2} = u_{\mathrm{m}}(t)\dot{x}(t) \\ P_{\mathrm{e}}(t) &= \frac{\bar{P}_{\mathrm{e}}(\bar{t})}{mw_{\mathrm{s}}^3 l_{\mathrm{s}}^2} = \frac{\bar{u}_{\mathrm{e}}(\bar{t})\bar{y}(\bar{t})}{mw_{\mathrm{s}}^3 l_{\mathrm{s}}^2} = \kappa^2 u_{\mathrm{e}}(t)\, y(t) \end{aligned} \tag{15}$$

In equation (15), the dimensional harvested power $\bar{P}_{\mathrm{h}}(\bar{t})$ is $\bar{y}^2(\bar{t})/R$ for a capacitive harvester and $R\bar{y}^2(\bar{t})$ for an inductive harvester. All the corresponding energies are nondimensionalized by the quantity $mw_{\mathrm{s}}^2 l_{\mathrm{s}}^2$. In the next section, the sliding mode control is applied to the bistable harvester described by these equations to move the harvester from a low-energy orbit or low-energy chaotic attractors to a high-energy orbit, and simulation results are presented.

4. Results and discussion

In this section, we apply sliding mode control with and without adaptation to the bistable system described earlier. For all the simulations we consider harmonic excitation of the form $F(t) = 0.08\sin(0.8t)$ with no disturbances. The low- and high-energy orbits for the uncontrolled system are achieved by initial conditions $[x, \dot{x}, y]^{\mathrm{T}} = [1, 0.5, 0]^{\mathrm{T}}$, and $[1, 1.3, 0]^{\mathrm{T}}$, respectively. The damping ratio and time constant ratio are set as $\zeta = 0.01$ and $\alpha = 0.05$. For the system without adaptation, we use parameters $\lambda = \eta_1 = \eta_2 = 1$; for the system with adaptation, these parameters are set to $\lambda = p_1 = p_2 = 1$ and $\eta_1 = \eta_2 = 0.1$.

Figure 1 shows time histories of the displacement and the electrical state of the bistable system driven by the harmonic excitation. The figure shows time histories of the low- and high-energy orbits as well as the low-energy orbit driven to high-energy orbit by the sliding mode control. In Figures 1 to 5, we assume that all the parameters are known and hence no adaptation is needed. Also, in the said figures a weak coupling ($\kappa^2 = 0.05$) is used for the simulations and the

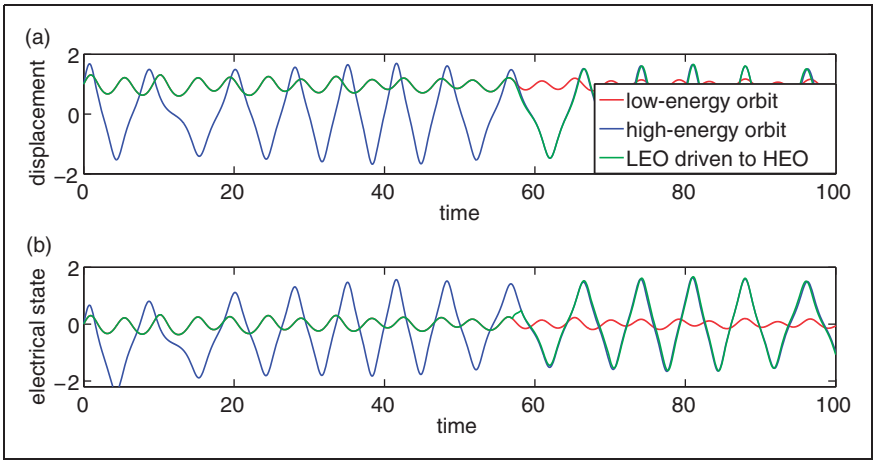

Figure 1. Time history of (a) the displacement and (b) the electrical state of the weakly coupled bistable harvester under harmonic excitation for the uncontrolled system in low- and high-energy orbits, as well as the controlled system driven from a low-energy orbit to a high-energy orbit.
HEO: high-energy orbit; LEO: low-energy orbit.

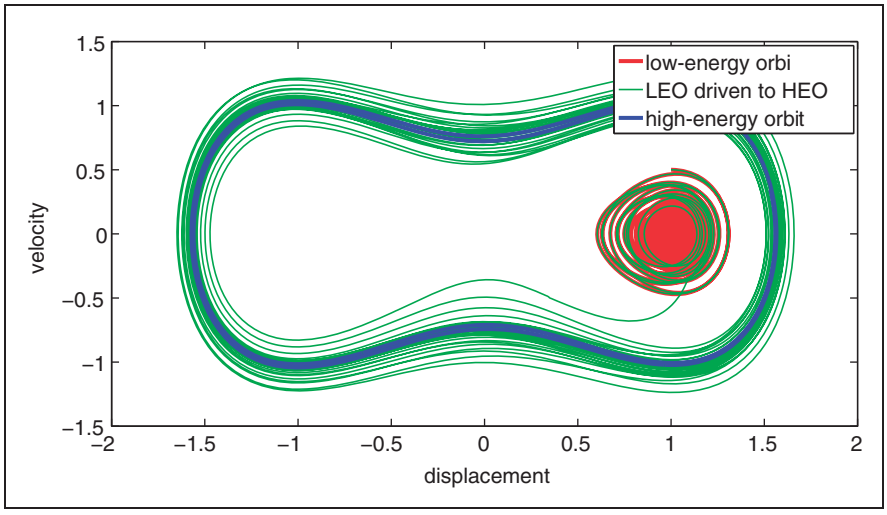

Figure 2. Velocity–displacement phase diagram of the weakly coupled bistable harvester under harmonic excitation for the uncontrolled system in low-energy and high-energy orbits, as well as the controlled system driven from a low-energy orbit to a high-energy orbit.
HEO: high-energy orbit; LEO: low-energy orbit.

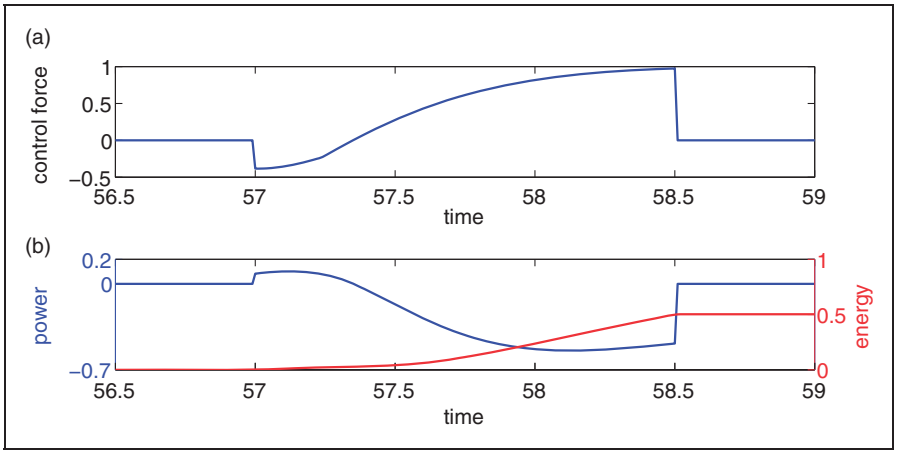

Figure 3. Time history of (a) the mechanical control force and (b) power and energy for the weakly coupled bistable harvester under harmonic excitation with sliding mode control entrainment in $t = [57, 58.5]$.

entrainment period (i.e. the time the controller is active) is set to $t = [57, 58.5]$. Figure 2 depicts Figure 1 as a phase diagram. Based on these figures, sliding mode control successfully entrains the system on the high-energy orbit to move the system response from the low-energy orbit to the high-energy orbit.

To check the feasibility of the implementation, the magnitude of the control forces should also be considered. Figures 3 and 4 depict the control force and its corresponding required power and energy in the mechanical and electrical domains, respectively. The magnitude of the mechanical control force u_{m} is about an order of magnitude larger than the excitation force. If the maximum attainable force is less than this, the control force could be clipped at the limit and applied for a longer entrainment period if necessary. The magnitude of the control forces could be adjusted and lowered by tuning the control parameters η_1, η_2, λ, and $\mathbf{P}$ but at the cost of a slower convergence to the sliding surface or a slower convergence to the desired trajectory once the system dynamics land on the sliding surface. It should also be noted that limiting the control force will most probably increase the minimum entrainment period; hence, despite the smaller control force, it might result in a decrease or increase of the overall control energy because of the longer entrainment period. This could be nicely cast as an optimization problem but is out of the scope of this study.

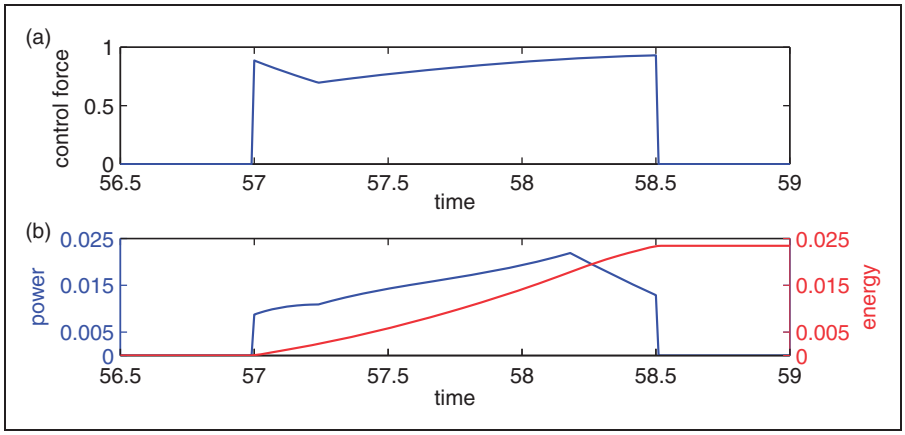

Figure 4. Time history of (a) the electrical control force and (b) power and energy for the weakly coupled bistable harvester under harmonic excitation with sliding mode control entrainment in $t = [57, 58.5]$.

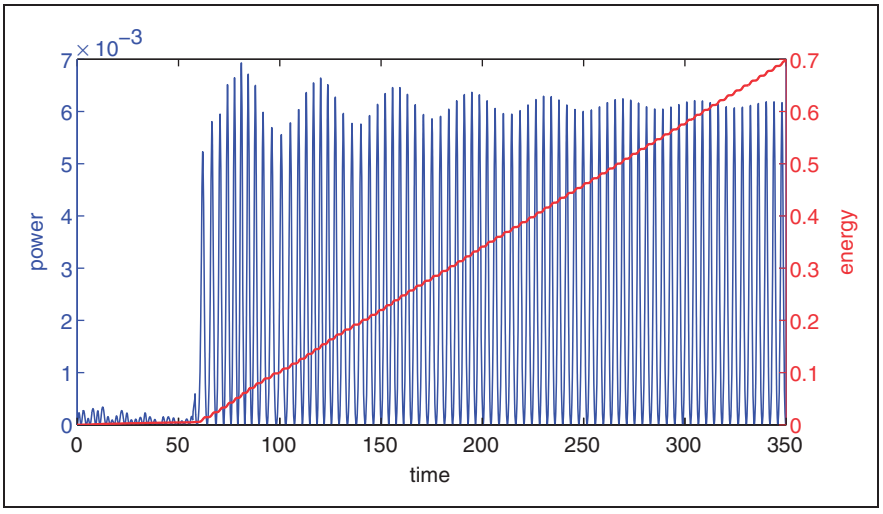

Figure 5. Time history of the harvested power and energy in the weakly coupled bistable harvester with sliding mode control entrainment in $t = [57, 58.5]$.

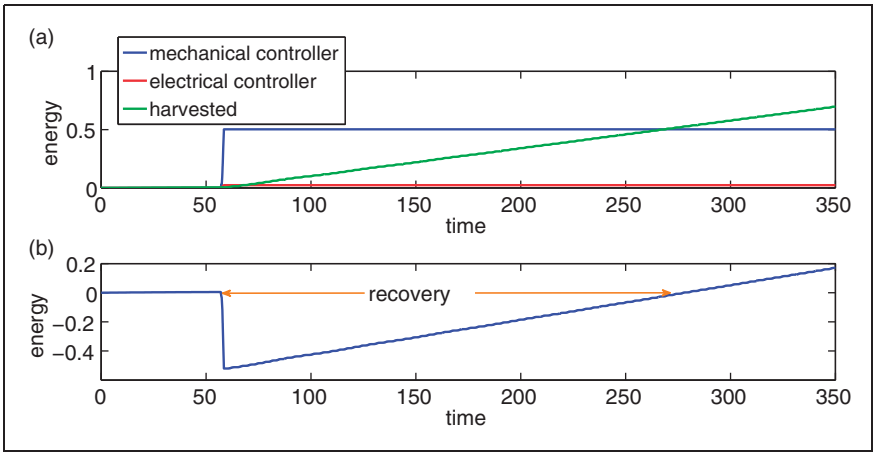

Figure 6. Time history of (a) the control and harvested energy and (b) the net harvested energy in the the weakly coupled bistable harvester with sliding mode control entrainment in $t = [57, 58.5]$.

Also, it could be seen that the energy required for the mechanical controller is significantly larger than the electrical controller. This is because the coupling is weak and the system response is dominated by the mechanical oscillator.

Figure 5 depicts the time history of the harvested power and energy. It can be seen that before the controller is turned on the system response is in the low-energy orbit and hence its corresponding harvested power and energy are significantly low whereas when the controller is turned on at $t = 57$ (for only 1.5 time units) the harvested power and energy are significantly improved. Figure 6(a) illustrates the harvested energy and the energy required for the mechanical and electrical controllers while Figure 6(b) shows the net harvested energy, i.e. the harvested energy minus the

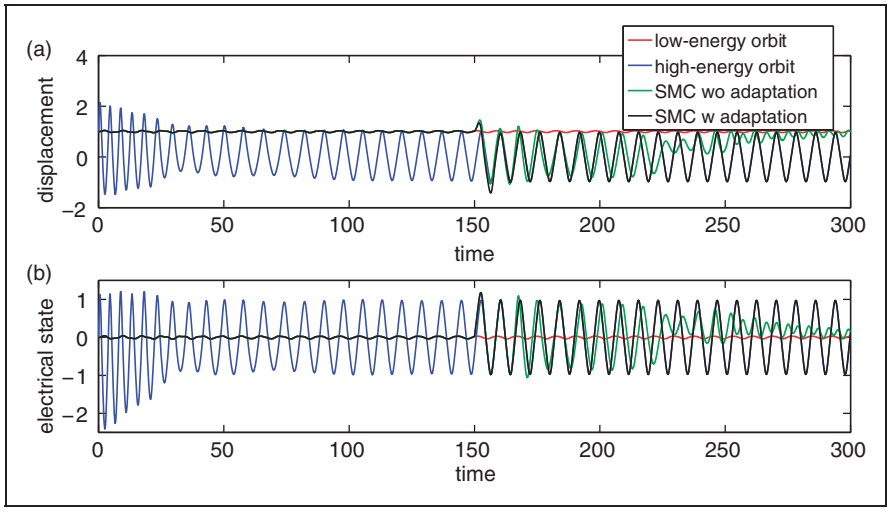

Figure 7. Time history of (a) the displacement and (b) the electrical state of the strongly coupled bistable harvester under harmonic excitation for the uncontrolled system in low-energy and high-energy orbits, as well as the controlled system driven from the low-energy orbit to high-energy orbit by sliding mode control with and without adaptation.
SMC: sliding mode control; w: with; wo: without.

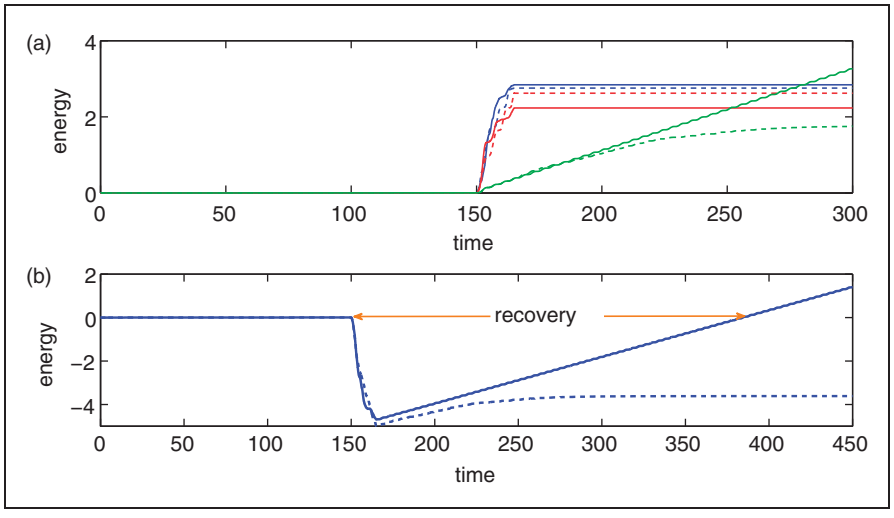

Figure 8. Time history of (a) the control and harvested energy and (b) the net harvested energy in the the strongly coupled bistable harvester with adaptive and nonadaptive sliding mode control entrainment in $t = [150, 165]$. Solid and dashed lines correspond to the controller with and without adaptation, respectively. Energy consumption of the mechanical and electrical controllers and the harvested energy in (a) are color coded blue, red, and green, respectively.

energy consumed by the controllers. It takes about 28 cycles of the excitation to recover the energy spent on the controllers.

We also consider the case where we have poor knowledge of the system parameters. In particular, we feed the controllers with incorrect information about the parameters ζ and κ^2. We set these parameters to 60% of their actual values, i.e. $\hat{\zeta} = 0.6 \times \zeta$ and $\hat{\kappa}^2 = 0.6 \times \kappa^2$. We consider a strong coupling with $\kappa^2 = 1$ in this case and we entrain the system for 15 time units in the period $t = [150, 165]$. Figure 7 illustrates the system response for sliding mode control with and without adaptation. According to Figure 7, the sliding mode control with adaptation adapts well to the incorrect parameters and maintains and entrains the system well on the high-energy orbit while the sliding mode control without adaptation fails to do so and, soon after the controller is turned off, the system converges back to the low-energy orbit. Figure 8 depicts the individual harvested and controller energy for the controlled system with and without adaptation as well as the net harvested energy. It can be seen from Figure 8(b) that the energy recovery takes place in about 29 cycles of the excitation force.

It is worth mentioning that with large control parameters, the sliding mode controller should be able to push the system response successfully from a low-energy to a high-energy orbit without adaptation *given* that the terms containing the uncertain parameters are bounded. This is true simply because given that these terms are bounded, they could be lumped into the terms pertaining to the unmodeled dynamics, i.e. d_1 and d_2. Large control parameters will result in faster and better convergence to the desired trajectory but at the same time will increase the consumed energy by the controllers; hence, at the very least, the adaptive sliding mode control will be a more energy-efficient controller than the nonadaptive one.

5. Conclusions

In this study, we proposed a novel robust and adaptive sliding mode control to control between the coexisting attractors in nonlinear systems, in particular, in nonlinear energy harvesters. The controller is robust to disturbances and unmodeled dynamics and adaptive to unknown system parameters. Based on the energy methods and Barbalat's lemma, given the desired trajectory, the proposed controller is proven to converge the system response from any arbitrary attractor to any desired attractor. The harvester model considered has generic coupling and nonlinearities in both mechanical and electrical domains. The external excitation is also deterministically generic. The control and adaptation laws are then applied to a specific design of energy harvesters: a bistable oscillator linearly coupled with a capacitive or inductive harvesting circuitry with a constant load resistance.

Simulation results show that the controller, via a short period of entrainment, can successfully push the system response from a low-energy to a high-energy orbit, and hence significantly improve the energy harvesting efficacy. In a weakly coupled harvester, the controller on the mechanical oscillator plays a crucial role, compared with the controller on the harvesting circuitry because of the dominance of the mechanical domain on the overall response of the system. Therefore, controlling only the mechanical oscillator is sufficient for the weakly coupled vibratory energy harvester. However, a long entrainment period is needed if the controller is applied only to the mechanical oscillator in a strongly coupled harvester. In a weakly coupled harvester, the mechanical control force is about 10 times larger than the excitation force in amplitude. If this is not realizable, the control force could be clipped at the maximum realizable force and instead applied for a longer entrainment period.

Simulation results also show that the sliding mode control with adaptation adapts well to the system parameters and successfully moves the system to the desired attractor even when knowledge of the system parameters is poor and incorrect, whereas the same controller without adaptation does not achieve the same with incorrect knowledge of the parameters. It is also shown that the energy consumed by the control forces is recovered in a reasonable time (in less than 30 cycles of the excitation). In conclusion, the proposed control method in this paper could be applied to a wide range of nonlinear harvesters with nonlinearity in either or both the mechanical and electrical domains in a very robust and adaptive fashion to ensure that the harvester is always operating in the desired high-energy orbit.

Declaration of Conflicting Interests

The author(s) declared no potential conflicts of interest with respect to the research, authorship, and/or publication of this article.

Funding

The author(s) received no financial support for the research, authorship, and/or publication of this article.

References

Daqaq MF, Masana R, Erturk A, et al. (2014) On the role of nonlinearities in vibratory energy harvesting: a critical review and discussion. *Applied Mechanics Reviews* 66(4): 040801.

Erturk A and Inman D (2011) Broadband piezoelectric power generation on high-energy orbits of the bistable duffing

oscillator with electromechanical coupling. *Journal of Sound and Vibration* 330(10): 2339–2353.

Geiyer D and Kauffman JL (2016) Control between coexistent attractors for optimal performance of a bistable piezoelectric vibration energy harvester. *SPIE Proceedings* 9799: 97990I.

Goswami B and Pisarchik AN (2008) Controlling multistability by small periodic perturbation. *International Journal of Bifurcation and Chaos* 18(06): 1645–1673.

Hosseinloo AH and Turitsyn K (2015a) Fundamental limits to nonlinear energy harvesting. *Physical Review Applied* 4(6): 064009.

Hosseinloo AH and Turitsyn K (2015b) Non-resonant energy harvesting via an adaptive bistable potential. *Smart Materials and Structures* 25(1): 015010.

Hosseinloo AH and Turitsyn K (2016a) Design of vibratory energy harvesters under stochastic parametric uncertainty: a new optimization philosophy. *Smart Materials and Structures* 25(5): 055023.

Hosseinloo AH and Turitsyn K (2016b) Optimization of vibratory energy harvesters with stochastic parametric uncertainty: a new perspective. *SPIE Proceedings* 9799: 97991L.

Hosseinloo AH, Vu TL, and Turitsyn K (2015) Optimal control strategies for efficient energy harvesting from ambient vibration. In: *IEEE 54th annual conference on decision and control (CDC)*, Osaka, Japan,15–18 December 2015, pp. 5391–5396. Piscataway, NJ: IEEE.

Jiang Y (1999) Trajectory selection in multistable systems using periodic drivings. *Physics Letters A* 264(1): 22–29.

Kumar A, Ali SF and Arockiarajan A (2016) Enhanced energy harvesting from nonlinear oscillators via chaos control. *IFAC-PapersOnLine* 49(1): 35–40.

Liu Y, Wiercigroch M, Ing J, et al. (2013) Intermittent control of coexisting attractors. *Philosophical Transactions of the Royal Society of London A: Mathematical, Physical and Engineering Sciences* 371(1993): 20120428.

Martinez-Zerega B, Pisarchik A and Tsimring L (2003) Using periodic modulation to control coexisting attractors induced by delayed feedback. *Physics Letters A* 318(1): 102–111.

Masuda A and Sato T (2016) Global stabilization of high-energy resonance for a nonlinear wideband electromagnetic vibration energy harvester. *SPIE Proceedings* 9799: 97990K.

Masuda A, Senda A, Sanada T, et al. (2013) Global stabilization of high-energy response for a duffing-type wideband nonlinear energy harvester via self-excitation and entrainment. *Journal of Intelligent Material Systems and Structures* 24(13): 1598–1612.

Ott E, Grebogi C and Yorke JA (1990) Controlling chaos. *Physical Review Letters* 64(11): 1196.

Pecora LM and Carroll TL (1991) Pseudoperiodic driving: eliminating multiple domains of attraction using chaos. *Physical Review Letters* 67(8): 945.

Pisarchik A (2001) Controlling the multistability of nonlinear systems with coexisting attractors. *Physical Review E* 64(4): 046203.

Pisarchik A and Goswami B (2000) Annihilation of one of the coexisting attractors in a bistable system. *Physical Review Letters* 84(7): 1423.

Slotine JJE and Li W (1991) *Applied Nonlinear Control*. Englewood Cliffs, NJ: Prentice-Hall.

Yang W, Ding M and Gang H (1995) Trajectory (phase) selection in multistable systems: Stochastic resonance, signal bias, and the effect of signal phase. *Physical Review Letters* 74(20): 3955.